Effect of Atmospheric Plasma Sprayed TiO₂–10% NiAl Cermet Coating Thickness on Cavitation Erosion, Sliding and Abrasive Wear Resistance

M. Szala [a,*], A. Dudek[b], A. Maruszczyk[c], M. Walczak[a,d], J. Chmiel[e] and M. Kowal[f]

[a]Lublin University of Technology, Faculty of Mechanical Engineering, Department of Materials Engineering,
Nadbystrzycka St. 36D, 20-618 Lublin, Poland

[b]Institute of Materials Engineering, Faculty of Production Engineering and Materials Technology,
Częstochowa University of Technology, Armii Krajowej St. 19, 42-200 Częstochowa, Poland

[c]Faculty of Mechanical Engineering and Computer Science, Częstochowa University of Technology,
Armii Krajowej St. 19, 42-200 Częstochowa, Poland

[d]University of Economics and Innovation in Lublin, Department of Mechanics and Mechanical Engineering,
Faculty of Transport and Computer Science, Projektowa St. 4, 20-209 Lublin, Poland

[e]Faculty of Engineering and Economics of Transport, Maritime University of Szczecin,
H. Pobożnego St. 11, 70-507 Szczecin, Poland

[f]Lublin University of Technology, Faculty of Civil Engineering and Architecture,
Nadbystrzycka St. 40, 20-618 Lublin, Poland

Atmospheric plasma spray (APS) wear-resistant coatings are popular in mechanical designing for increasing the operation time of machine elements. APS enables the deposition of ceramic, metallic, and cermet coatings to ameliorate the effects of wear that cause most of the failures of machine elements. The aim of the paper was to investigate the influence of the coating thickness of TiO₂–10 wt% NiAl on abrasive, sliding, and cavitation erosion resistance. Titania based coatings were deposited by means of APS onto a mild steel substrate using TiO₂–10 wt% NiAl feedstock material. The coatings had thicknesses of approximately 50, 100, and 200 μm. The morphology and microstructure of the coatings were examined using a light optical microscope (LOM) and scanning electron microscope (SEM). The as-deposited surface topography and hardness of the coatings were determined. The porosity and thickness were evaluated by using quantities image analysis software. Cavitation erosion tests were performed according to ASTM G32 (vibratory apparatus) and ASTM G134 (cavitating liquid jet). Abrasive and sliding wear tests were conducted using a three body abrasive tester and ball-on-disc apparatus, respectively. Generally the thickest coating presents an increase in resistance to sliding wear and cavitation erosion over the thinnest cermet coating.

1. Introduction

Atmospheric plasma spray (APS) wear-resistant coatings are commonly used in mechanical designing to increase the operation time of machine elements since most failures are an effect of wear. It is widely known that the APS process relies on a strong electric arc generated between a positively charged pole (anode) and a negatively charged pole (cathode). This ionizes the flowing process gasses into the plasma state. Powdered feedstock material is injected into the plasma jet. The plasma melts the powder particles and propels them onto the workpiece surface [1–4]. The APS process is widely applicable not only for ceramic (e.g. containing: Al_2O_3, $TiO_2Cr_2O_3ZrO_2$ [2,4–7]) or metallic (e.g. FeCrC,

CoCrW, NiAl, NiCrBSi [3,4,8,9]) based coatings, it also enables deposition of the composite system of ceramics and metallic phases which are known as cermets [10]. In addition, the deposition of cermet coatings is beneficial especially in the cases where ceramic coatings improvement of bond strength, impact strength, or shock resistance are needed.

The literature survey indicates that titania (TiO_2) based coatings can be produced by the APS process and that they possess a high degree of hardness, high density, good ductility, and good adhesive bonding to the substrate. Plasma sprayed TiO_2-containing composite coatings have been used to resist abrasive, fretting, cavitation, and erosive wear [6, 11]. TiO_2–10 wt% NiAl cermet coatings have a unique composition and limited information is available in the literature [8]. However, the structure of the coating produced as cermet, that contains TiO_2 and NiAl, was not completely examined. In addition, the literature survey indicates that cavitation, sliding, and abrasion wear resistance of TiO_2–10 wt% NiAl

---

*corresponding author; e-mail: m.szala@pollub.pl

coating has not been investigated. Moreover, testing the effect of coating thickness in relation to the optimization of coating spraying parameters, coatings structure, or studying the influence of coating thickness on functional properties (i.e. wear resistance) of plasma spray coatings is still a relevant problem and is the subject of many papers [1, 2, 5, 6, 12, 13].

The aim of this study is to investigate the effect of the thicknesses of TiO_2-NiAl coatings on abrasive, sliding, and cavitation wear resistance.

2. Materials and methods

TiO_2–10 wt% NiAl coatings were deposited using atmospheric plasma spray (APS) by means of a Plamotron PN-200 facility onto the workpiece surface made of low alloy steel grade 40Cr4. The coating thicknesses equalled approximately 50 μm, 100 μm, and 200 μm and the deposition parameters were given in our earlier paper [8]. The coating microstructure was analyzed using a light optical microscopy (Axiovert 25, Carl Zeiss) and a scanning electron microscope (SEM, JSM-6610LV, JEOL). The structures were studied using metallographic cross-sectional coating samples. Porosity, thickness, and metallic to ceramic ratio were determined with light microscopy images of cross-sections via the image analysis software ImagePro (Media Cybernetics, Inc., USA). Furthermore, microhardness measurements with Knopp harnesses (HK) were determined as an average value of 10 measurements using a microhardness tester (FM-800, FutureTech).

A set of three APS sprayed specimens designated 50, 100, and 200 with coating thicknesses of 50 μm, 100 μm and 200 μm, respectively, were put into cavitation, sliding, and abrasive wear testing. The cavitation tests were conducted on two types of test stand: an ultrasonic test stand (G32) and cavitation liquid (G134). The ultrasonic tests were conducted using the apparatus conforming the ASTM G-32 [14] standard recommendations, according to an alternative stationary specimen method which is dedicated to coatings testing with standoff 1 mm and 15.8 mm diameter sonotrode tip. Details of the cavitation procedure are given in [15, 16]. The cavitation liquid jet test was conducted in accordance with the ASTM G134 [17] standard procedure using the test stand described in [18]. The test parameters were: jet pressure 12 $\pm$ 0.2 MPa; ambient pressure 0.2 $\pm$ 0.02 MPa; nozzle diameter 0.4 mm; jet velocity 500 $\pm$ 10 m/s; temperature 24 $\pm$ 1 °C; and a standoff distance of 14 mm. Compared to the ultrasonic horn testing (G32), the cavitation generated by a cavitating jet (G134) provides more realistic cavitation bubble clouds than those produced by an ultrasonic horn, and test conditions are more relevant to the real flows [19]. The abrasive wear test was evaluated using a rubber-wheel abrasion test with the test stand described in [20]. The test was conducted with the coarse-grained abrasives corundum grain size approximately 80–200 μm. The total duration of the test

was 90 s with an applied rubber-wheel to specimen force of 22 N. The sliding wear test was conducted with usage or on a "ball-on-disc" tribotester manufactured by CSM Instruments at room temperature under dry friction conditions. Balls with a diameter of 6 mm made of 100Cr6 (manufactured by CSM Instruments) were used as a counter-sample (ball). The tests were carried out under a load of 10 N with a linear speed of 5 cm/s on a radius of 3 mm. The total test distance was equal to 300 m and it was used to record the friction coefficient and procedure of sliding test results evaluation. The computation of wear factor is described in [21, 22]. The worn samples wear traces were assessed with a scanning electron microscope Phenom Pro-X (15 kV, BSE detector and SEM-topo mode, Phenom-World), using a stereoscope microscope (Nikon SMZ 1500, Nikon Corporation), by means of a Contour GT profilometer (manufactured by Bruker, Germany). Time-erosion cavitation curves were plotted by means of measuring the mass loss of the tested samples with an accuracy of $\pm$0.1 mg. In wear testing the reference samples were mild steel grade C45 and aluminum alloy PA2 (AlMg2).

3. Results and discussion

Considering the fact that the wear resistance of coatings were derived from structure and properties, metallography, topography, and hardness investigations were carried out on homogeneity of the as-sprayed coatings. The properties of the coatings are summarized in Table I. From the blend of TiO_2–10 wt% NiAl feedstock powder, three APS cermet coatings were sprayed to obtain different thicknesses (approximately 50, 100, and 200 μm, see Table I). Structural investigations allow for the identification of the typical lamellar structure of thermally sprayed cermet coatings [10, 15] containing unmelted particles, ceramic and metallic lamellas, lamella interfaces, porosity, oxide particles, and microcracks which can be seen in Fig. 1. The two main phases in the structure were recognized as ceramic and metallic. The previous SEM-EDS studies [8] conducted for the as-sprayed coating structure, acknowledged that the phase, visible in the gray colour in Fig. 1, was mainly formed from TiO_2 ceramics and the lamellas visible in the white colour derives from metallic NiAl material. Each coating surface morphology, structure, and hardness value was compared to the other two specimens, even though the coatings were deposited with different thicknesses, see Table I. Both the Ra and Rz measured roughness parameters of as-sprayed TiO_2–10 wt% NiAl coating surfaces were at a comparable level to each investigated coating (Table I) and were lower than the roughness $Ra = 14$–23 μm of 100% TiO_2 coatings presented in [2]. In addition, the mean hardness of the coatings was at a level of 600 HK (approximately 566 HV) which is below the range of TiO_2 hardness given as 680 HV [6].

Coatings characterization

Coating code	Coating thickness [μm]	Surface roughness parameter [μm]		Porosity [%]	Metallic lamellas [%]	Hardness (HK)
		Ra	Rz			
50	47 ± 6.6	3.18	17.92	5.3 ± 0.9	7.5 ± 0.5	
100	117 ± 8.8	3.58	18.77	4.7 ± 0.6	8.3 ± 0.7	600 ± 14
200	225 ± 10.2	3.20	19.67	4.5 ± 0.8	8.9 ± 0.5	
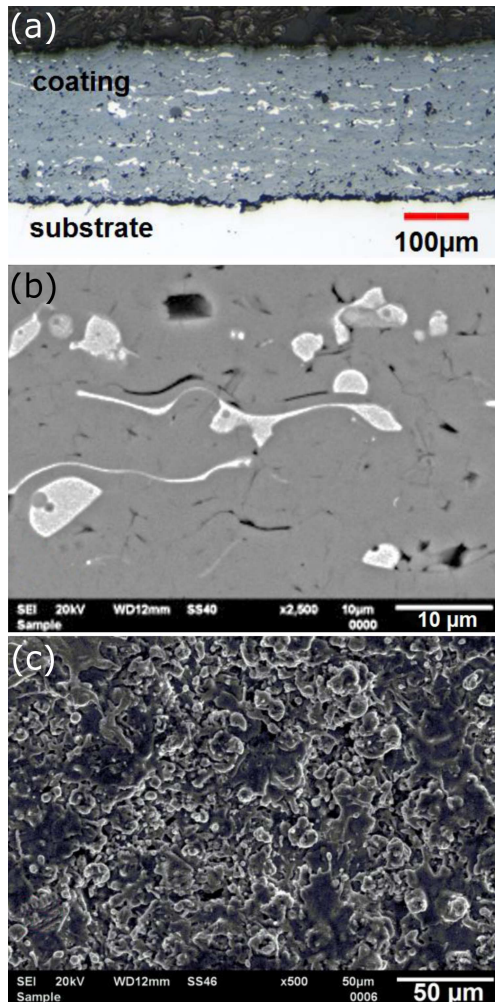
Fig. 1. Microstructure of cermet TiO₂–10% NiAl (a) coating cross-section, LOM; (b) SEM micrographs of structure and (c) as-sprayed coating surface.

Similarly, the porosity value of the cermet coatings was at a level of about 5% which is a higher value than the porosity of TiO₂ coatings reported in [6] at a level of 2%. Hardness and porosity are strongly affected by the spraying parameters. [1, 5, 23] as well as by the NiAl metallic lamellas content. Furthermore, the literature denoted an increase in porosity with the increasing coating thickness [24] which is in contrast to the results obtained by our study. An examination of the computation conducted by image analysis found no visible relationships of thickness with porosity, hardness, or surface roughness.

This confirms the homogeneity of the coatings investigated in our study. A comparable analysis of coating characteristics produced evidence that coating thickness does not affect structure and properties. This is derived from the fact that the coatings were manufactured with the same plasma deposition parameters.

The abrasion, sliding, and cavitation wear testing results are presented in Figs. 2 and 3 and in Table II. The abrasion test (see Fig. 2) confirmed that TiO₂–10 wt% NiAl coatings present a mass loss almost three times lower than the reference mild steel grade C45. The thermally sprayed coatings material loss was at a similar level, Fig. 2 Scanning electron microscopy observations of wear traces (Fig. 4) conducted in the BSD and SEM-topographic modes indicate that the NiAl splats abrasive wear mechanism was due to microploughing and microcutting while the prevailing wear mechanism of ceramic splats was microcutting resulting in the spallation of the splats. The results obtained during the sliding wear tests are given in Fig. 5 and Table II. Coating 200 presents the highest sliding wear resistance, even higher than that calculated for reference C45. The computed mean wear factor decreases with the increase in coating thickness (see Fig. 5). The friction coefficient of as-sprayed coatings is at the same level. In addition, it is lower than the friction coefficient of C45 steel (Table II). The friction coefficient did not correlate with the coating thicknesses. The general influence of cermet TiO₂–10 wt% NiAl coating thickness on wear resistance was identified. On the whole, the thickest coating 200 presents higher mean wear resistance to abrasion and sliding wear than the thinnest coating (coating 50).
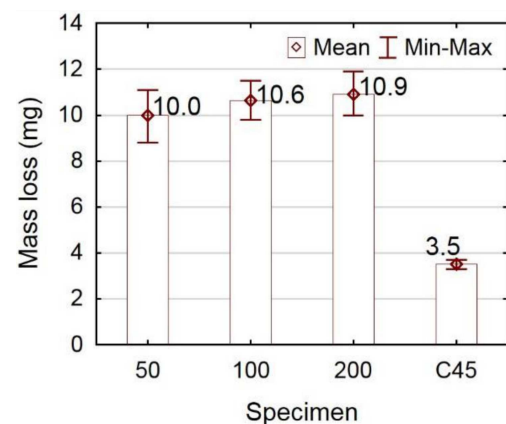
Fig. 2. Abrasive wear results.
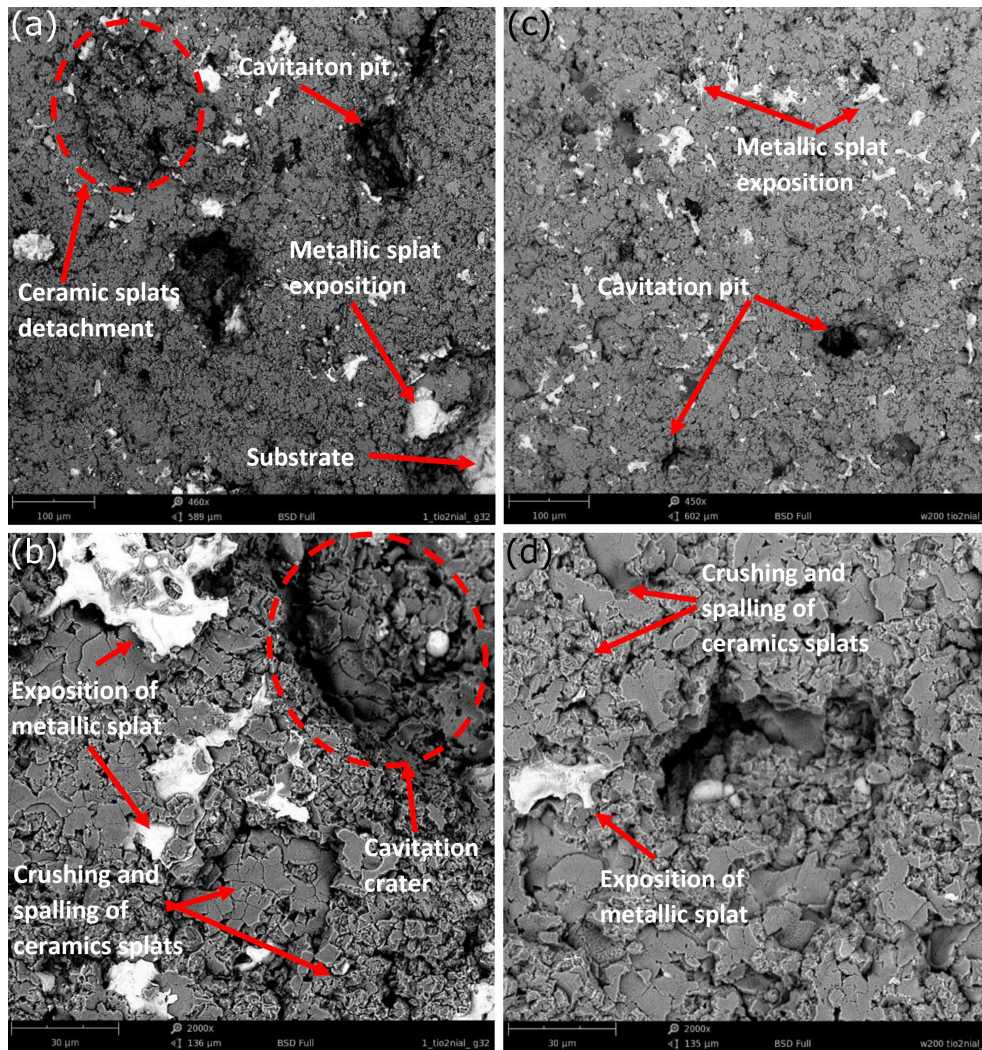
Fig. 3.   Coatings surface worn by cavitation erosion in G32 (a, b) and G134 (c, d) test method, SEM.
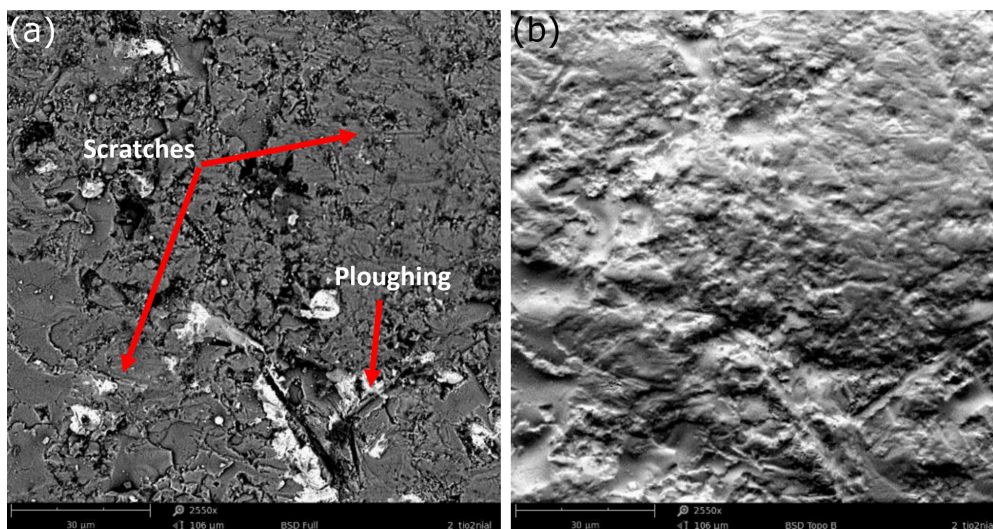
Fig. 4.   Wear trace visible on the surface of coating 200 after abrasive testing, SEM BSD (a) and SEM-topo (b).
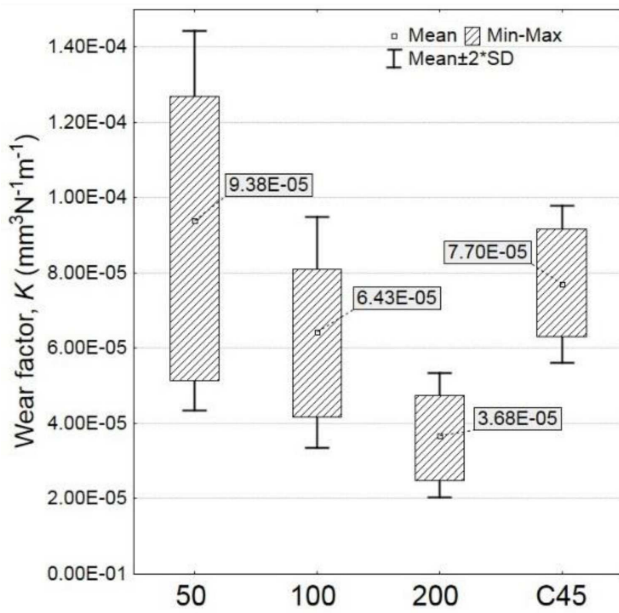
Fig. 5. Ball-on-disc sliding test results of coatings and reference alloy.

Fig. 6. Cavitation erosion curves obtained in: (a) vibratory testing, (b) cavitation liquid jet testing.

TABLE II

Friction coefficient measured in sliding test

Specimen	Friction coefficient	
	Mean	SD
50	0.773	0.094
100	0.763	0.106
200	0.718	0.055
C45	0.660	0.046

Cavitation erosion curves are plotted in Fig. 6, and the exemplary wear micrographs are given in Fig. 3. Cermet TiO₂–10 wt% NiAl coatings present lower resistance to cavitation than bulk metal alloys (C45 or PA2). While reading the cavitation curves of metal alloys, the incubation period of cavitation erosion and non-constant cavitation erosion rate are usually evident [25, 26]. Thus the main difference in the cavitation erosion process of the ceramic-based coatings and metal alloys consists of the evident incubation stage of cavitation erosion identified for the reference PA2 and C45 samples and the negligible incubation period of cavitation erosion visible for the sprayed coatings (see Fig. 6). Additionally, a constant erosion rate is acknowledged for the thermally sprayed TiO₂–10 wt% NiAl coatings. These findings are in agreement with the results presented for the flame-sprayed Al₂O₃–40% TiO₂/NiMoAl cermet [15].

Stereoscope microscopy observations of surface coatings conducted at different time intervals allow for identification of the growth of cavitation pits in shorter periods of time for coating 50 than for coatings 100 and 200.

Arisen pits affect the acceleration of mass loss due to coating material detachment of coarse chunks. Hence, both the delamination of coating 50 after 15 min of testing (Fig. 6a) and the increase in mass loss observed after 30 min of cavitation (Fig. 6b) were the result of the coating penetration by pits (pit growth) and subsequent coating material detachment. While comparing the mass loss of the tested specimens given in Fig. 6 and worn surfaces given in Fig. 3, it may be concluded that the cavitation load generated by the vibratory facility (G32) is higher than that for the liquid jet (G134). This is confirmed by the fact that cermets tested in the vibratory apparatus (Fig. 3a and b) present deeper pits on the surface, correspondingly, the fragmentation of ceramic lamellas is much more severe than that observed for the coatings tested according to the G134 facility, given in Fig. 3b and d.

As mentioned above, despite different thicknesses, the coatings present a uniform lamellae structure, typical of the APS-deposited material. The conducted analysis of SEM micrographs acknowledged that the dominant mechanism of cavitation erosion of APS TiO₂-NiAl coatings is brittle fracture starting at the edges of ceramic lamellas and splat initial cracks in ceramic lamellas, which result in coating material removal. That cavitation erosion mechanism is typical of thermally sprayed ceramic-rich coatings [15, 27, 28]. Moreover, in the case of our study the ceramic was enriched with metallic splats that seemed beneficial for preventing the detachment of the ceramic (Fig. 3b and d) while erosion started in the regions depleted with metallic splats. Once the ceramics were spalled, metallic splats, anchored in the ceramic matrix, were extracted with chunks of the coating material.

It can be concluded that even though no close relationship between the coating thickness and wear resistance was identified, generally the thickness of coatings affects wear resistance. On the whole, the thinnest coating (marked as 50) presents the lowest mean values of resistance to abrasion, sliding, and cavitation erosion measured with a vibratory rig. It seems that thicker coatings (marked as 100 and 200) present better wear resistance

than coating 50. Thus in liquid jet testing it was found that the thickest coating (200) presents the lowest mass loss. The results of cavitation tests indicate that the thick coating (200) accumulates cavitation loads better than the thinner coating 50. The thicker deposited layer of coating materials prevents pit growth toward the substrate and final detachment from the substrate.

4. Conclusions

In this paper the atmospheric plasma sprayed (APS) cermet TiO_2–10% NiAl were deposited with the coating thicknesses of approximately 50, 100, and 200 μm. The influence of coating thickness on the structure and properties of the coating and on the results of sliding, abrasion, and cavitation erosion tests were investigated. The following conclusions were drawn:

1. Conducted comparable analyses of atmospheric plasma sprayed TiO_2–10% NiAl coatings characteristics allow for the statement that the coatings present a homogeneity of structure and properties even though cermet coatings average thickness equals approximately 50, 100, and 200 μm. The thickness does not affect TiO_2–10% NiAl cermet porosity, hardness, and surface roughness.

2. Cermet TiO_2–10% NiAl coatings exhibit lower abrasion and cavitation erosion resistance than the reference materials. In the sliding wear test, a 200 μm thick coating presents better wear resistance than steel C45.

3. It can be concluded that even though no strong relationship between the coating thickness and wear resistance was identified, generally the thickest coating presents an increase in sliding and cavitation erosion resistance compared to the thinnest cermet coating.

4. The abrasive wear mechanism does not rely on the thickness of cermet TiO_2–10% NiAl coatings and wear of metallic splats was due to microploughing and microcutting while the prevailing wear mechanism of ceramic splats was microcutting.

5. It was observed that the mechanism of cavitation erosion of TiO_2–10% NiAl cermet consists in ceramic lamellas brittle cracking, alternate removal of ceramic and metallic splats combined with pit growth as well as subsequent coating material detachment from the substrate.

6. The coating thickness has a beneficial effect on the deceleration of the process of cavitation erosion mass loss by slowing down the growth of the cavitation pits toward the substrate and preventing the coating material from massive chunk detachment.

References

[1] P. Sokołowski, P. Nylen, R. Musalek, L. Łatka, S. Kozerski, D. Dietrich, T. Lampke, L. Pawłowski, *Surf. Coat. Technol.* **318**, 250 (2017).

[2] A. Berkath Ali Khan, C.C. Anil Kumar, M. Suresh P, *Int. J. Innov. Res. Sci. Eng. Technol.* **3**, 179 (2014).

[3] J.R. Davis, *Handbook of Thermal Spray Technology*, ASM International, OH, USA, 2004.

[4] Atmospheric Plasma Spray, 2018.

[5] L. Łatka, A. Cattini, L. Pawłowski, S. Valette, B. Pateyron, J.P. Lecompte, R. Kumar, A. Denoirjean, *Surf. Coat. Technol.* **208**, 87 (2012).

[6] S.Y. Jiang, H.J. Xie, *Proc. Inst. Mech. Eng. Part J J. Eng. Tribol.* **225**, 128 (2011).

[7] G. Guidoni, A. Dudek, S. Patsias, M. Anglada, *Mater. Sci. Eng. A* **397**, 209 (2005).

[8] A. Maruszczyk, A. Dudek, M. Szala, *Adv. Sci. Technol. Res. J.* **11**, 204 (2017).

[9] S. Dong, B. Song, H. Liao, C. Coddet, *Surf. Coat. Technol.* **268**, 36 (2015).

[10] R. Unabia, R. Candidato, L. Pawłowski, *Metals* **8**, 420 (2018).

[11] W.W. Dai, C.X. Ding, J.F. Li, Y.F. Zhang, P.Y. Zhang, *Wear* **196**, 238 (1996).

[12] H.M. Choi, B.S. Kang, W.K. Choi, D.G. Choi, S.K. Choi, J.C. Kim, Y.K. Park, G.M. Kim, *J. Mater. Sci.* **33**, 5895 (1998).

[13] D. Tang, *IOP Conf. Ser. Mater. Sci. Eng.* **87**, 012097 (2015).

[14] *ASTM G32-10: Standard Test Method for Cavitation Erosion Using Vibratory Apparatus*, ASTM International, West Conshohocken (PA) 2010.

[15] M. Szala, T. Hejwowski, *Coatings* **8**, 254 (2018).

[16] M. Szala, T. Hejwowski, I. Lenart, *Adv. Sci. Technol. Res. J.* **8**, 36 (2014).

[17] *ASTM G134-95 Test Method for Erosion of Solid Materials by Cavitating Liquid Jet*, ASTM International, 2010.

[18] J. Chmiel, *Rola synergizmu i krótkookresowych zjawisk elektrochemicznych w rozwoju niszczenia erozyjno-kawitacyjnego materiałów metalowych*, Wydawnictwo Naukowe Akademii Morskiej, 2015 (in Polish).

[19] K.H. Kim, G. Chahine, J.P. Franc, A. Karimi, *Advanced Experimental and Numerical Techniques for Cavitation Erosion Prediction*, Springer, Netherlands 2014.

[20] T. Hejwowski, *Vacuum* **83**, 166 (2008).

[21] M. Walczak, D. Pieniak, M. Zwierzchowski, *Arch. Civ. Mech. Eng.* **15**, 116 (2015).

[22] M. Walczak, K. Drozd, *Curr. Issues Pharm. Med. Sci.* **29**, 158 (2016).

[23] S.M. Forghani, M.J. Ghazali, A. Muchtar, A.R. Daud, N.H.N. Yusoff, C.H. Azhari, *Ceram. Int.* **39**, 3121 (2013).

[24] M. Öksüz, H. Yıldırım, S. Erturan, *J. Appl. Polym. Sci.* **100**, 3609 (2006).

[25] M. Szala, B. Dybowski, T.J. Hejwowski, A. Kiełbus, *Solid State Phenom.* **229**, 99 (2015).

[26] J. Chmiel, R. Jasionowski, D. Zasada, *Solid State Phenom.* **225**, 19 (2015).

[27] V. Matikainen, K. Niemi, H. Koivuluoto, P. Vuoristo, *Coatings* **4**, 18 (2014).

[28] K. Jafarzadeh, Z. Valefi, B. Ghavidel, *Surf. Coat. Technol.* **205**, 1850 (2010).